


ORIGINAL RESEARCH

Sustainable Energy

Synthesis and photoelectrochemical performance of Co doped SrTiO₃ nanostructures photoanode

Arti Mishra^{1,2} | Hemalatha Parangusan¹ | Jolly Bhadra¹  | Zubair Ahmed¹ |
Shoaib Mallick¹ | Farid Touati³ | Noora Al-Thani¹

¹Qatar University Young Scientists Center (QUYSC), Qatar University, Doha, Qatar

²Center for Advanced Materials (CAM), Qatar University, Doha, Qatar

³Department of Electrical Engineering, College of Engineering, Qatar University, Doha, Qatar

Correspondence

Jolly Bhadra, Qatar University Young Scientists Center (QUYSC), Qatar University, Doha, Qatar.

Email: jollybhadra@qu.edu.qa

Funding information

Qatar University, Grant/Award Number: QUCG-CAM-20/21-6

Abstract

It is pertinent to realize that scientific research indicates that the most promising method for producing H₂ is photo electrochemical water splitting through a photo anode. Cobalt-doped SrTiO₃ (Co-SrTiO₃) composite nanostructures were created in this study via hydrothermal synthesis. The impact of cobalt concentration change on Co-SrTiO₃ has been identified using morphological, structural, and photo electrochemical research. Surface morphology of pure SrTiO₃ nanoparticles using SEM and TEM reveals that the particles are intermittently agglomerated. The inclusion of Cobalt lowered the particle size of the nanostructures to 23 nm than pure SrTiO₃ (41 nm). In addition, the peak profile has been influenced by cubic phase also identified from the x-ray diffraction analysis. The purity and composition of the materials were revealed by XPS analysis. The Co-SrTiO₃ composite's produced the best charge transfer and recombination capabilities at 3% Co doping, according to electrochemical chemical impedance (EIS) spectroscopy. At 0.2 V applied potential, the obtained 3% Co-doped SrTiO₃ photoanode system displays a photocurrent density of around 3.45 mA/cm². The outcomes show that a promising application for the Co-doped SrTiO₃ photoanode in photoelectrochemical water splitting.

KEYWORDS

cobalt, photocatalyst, strontium Titanate, water splitting

1 | INTRODUCTION

Despite beginning in the 1990s, the EU adopts a hydrogen economy policy around 2010, followed by third-world economies, and active exploitation of renewable sources (Solar, Wind, and Hydro) of energy are the only solution for global energy crisis and environmental problems.¹ In this context photoelectrochemical water splitting (PEC) has been found most promising process to convert solar energy in the form of hydrogen.² However, synthesis of nanomaterial with controlled size and high photochemical properties using various semiconductors has been always challenging. In this context SrTiO₃ materials with

perovskite structure are very useful owing to their valence and vacancy control, thermal stability, and lower photocorrosion.³ However, due to charge recombination produced by surface states, SrTiO₃ has a low photogenerated current density and poor light absorption due to a wide band gap (3.2 eV). To address this issue, several approaches have been proposed, including nanostructure manipulation, elemental doping, and cocatalyst loading. Doping is one of the most common method to increase the photo conductivity and carrier concentration of SrTiO₃.⁴

It has been reported that the photoconductivity is increased with the increase of platinum doping and the presence of platinum also decreasing the crystallite size. In a recent research Lanthanum and

This is an open access article under the terms of the [Creative Commons Attribution](https://creativecommons.org/licenses/by/4.0/) License, which permits use, distribution and reproduction in any medium, provided the original work is properly cited.

© 2023 The Authors. *Environmental Progress & Sustainable Energy* published by Wiley Periodicals LLC on behalf of American Institute of Chemical Engineers.

Rhodium doped SrTiO₃ have demonstrate high photo catalytic activity under phosphate buffered electrolyte solution.^{4,5} Addition of Lathanum and Rhodium on the SrTiO₃ surface and surface modification accelerates the supply of reactants to active sites and is more effective to enhancing the photocatalytic activity. The tungsten doping in SrTiO₃ has been done using sonication assisted solid state method and it has shown very high crystalline nature of synthesized material.⁶ When tungsten was doped into SrTiO₃ surface, the band gap was decreased compared to the pure SrTiO₃ sample and its electrical conductivity was increased, which can be utilized for the solar cell devices. Palladium (Pd) nanoparticle doping in SrTiO₃ has been performed using photochemical deposition and it has been improved visible and near infrared charge separation efficiency significantly and it generated more active radicals, which led to an enhanced photocatalysis performance.⁷ It has been proven that transition metal doping improves optoelectronic properties of perovskite materials by modifying their electrocatalytic capabilities and resultant materials are suitable for electrochemical reactions with molecular oxygen,⁸ when Sr, Fe, and Co doped with non-noble metal perovskite LaNiO₃ and LaFeO₃ produced higher oxygen evolution reaction (OER).⁹ Flores et al. modified ABX₃ structure of perovskite and shown that large cation A were found to predominate at the surface of the catalyst; nevertheless, strong substitution with cobalt leads to enrichment of the cations in their respective higher oxidation states (A⁴⁺ and Co³⁺ instead of A³⁺ and Co²⁺) at the surface.¹⁰ In this work, the transition metal cobalt was doped with SrTiO₃ perovskite.

The hydrothermal process offers a number of benefits, one of which is a reduced need for energy due to the low temperature needs (less than 250°C). In addition, the amount of transformation as well as the size of the newly manufactured crystal may be controlled by the amount of reaction time as well as the temperature during the hydrothermal process. Recently Tezcan et al. utilized hydrothermal process and synthesized CdS Quantum Dots (QD) on a FTO glass, coated with TiO₂ nano rod arrays (NRAs) and Ag deposited. LSV studies reveal that bare TiO₂ NRAs display 0.17 mA/cm², which increased to 0.623 mA/cm² using CdS QDs and improved to 0.931 mA/cm² with Ag nanoparticles at 1.23 V_{RHE}.¹¹ LimHet al. prepared hydrothermally SrTiO₃ nano cubes, Pd nanoparticles are photochemically deposited on SrTiO₃ to improve visible and near infrared region photon absorption.⁷ Mone et al. synthesized Sn₃O₄ nanowires of 2.55 eV bandgap and used H₂S electrolyte for H₂ generation, the experiment has demonstrate under natural sunlight conditions.¹² The main task of photocatalysis are to increase the conversion rate and utilization coefficient of solar energy. In this context Xia et al. synthesized cadmium sulfide nanoparticles (CdS NPs) on 2D zinc porphyrin nanosheets (Zn-TCPP NSs)¹³ similarly Chen et al. synthesized Sb₂S₃/CdS/CdIn₂S₄ cascaded to address problem of charge separation and recombination.¹⁴ Three dimensional branches of TiO₂ (B-TiO₂) photoanode has been synthesized using hydrothermal process, NiOOH act as co-catalyst with an ultrathin Al₂O₃ passivation layer. The results have been shown that B-TiO₂/Al₂O₃/NiOOH heterojunction provide very high interface between catalyst and photo electrode.¹⁵ Hence here we have utilized hydrothermal method to synthesize Co-SrTiO₃, and it was demonstrated that the resultant exhibited a greater photocurrent density than the pure SrTiO₃.

2 | EXPERIMENTAL PROCEDURE

2.1 | Materials

Strontium acetate (C₄H₆O₄Sr), titanium (IV) n-butoxide ((C₁₆H₃₆O₄ Ti), Cobalt acetate (C₄H₆CoO₄) were purchased from Sigma-Aldrich. ethanol (C₂H₅OH) was purchased from Sigma Aldrich. All the chemicals were of analytical grade and used without further purifications.

2.2 | Preparation of SrTiO₃ and Co-doped SrTiO₃ photocatalyst

In a typical procedure, the Ti Source is titanium (IV) n-butoxide (1 mL) was added dropwise into ethanol (25 mL) under magnetic stirring at room temperature. The suspension was added into 25 mL of an aqueous solution containing 5 mmol Sr is from Strontium acetate. Then, the suspension was poured into a stainless steel Teflon-lined autoclave for hydrothermal treatment. For the synthesis of Co-doped SrTiO₃, required amount of C₄H₆O₄Sr and C₁₆H₃₆O₄ and C₄H₆CoO₄ with different mol % of Co ions (1%, 3%, and 5%) were prepared by hydrothermal method.¹⁶ The Sr and Co precursors were dissolved in deionized water. Then, Ti precursor was dissolved in ethanol. Both solutions are stirred for 2 h until a homogeneous solution was obtained. The pH is adjusted at 13 by adding the KOH solution (0.1 M). The whole solution after stirring was transferred to an autoclave at a temperature of 180°C for 24 h. Finally, the resultant material was filtered and the precipitate was washed in distilled water and ethanol. The final powder was obtained after drying at 80°C for 6 h and its corresponding schematic synthesis process is illustrated in Figure 1.

2.3 | Material characterization

X-ray diffraction studies were performed by XRD diffractometer (Empyrean, Panalytical, UK). The surface morphologies were analyzed through scanning electron microscope (FE-SEM, XL-30E Philips Co., Holland), and transmission electron microscopy (TEM, Phillips CM 12) respectively. The functional groups on the surface were measured by an Kratos AXIS Ultra DLA x-ray photoelectron spectroscopy. Biocrom Libra S 70 UV-vis spectrometer (UV-vis absorbance spectra). The photocatalytic performance of as-obtained photoelectrodes were performed in a typical three-electrode electrochemical workstation with 1 M KOH was used as an electrolyte under simulated solar light irradiation (Oriel, 450 W Xenon, AAA class). First, under ultrasonic stirring, 5 mg of pure SrTiO₃ and Co-doped SrTiO₃ powder were dissolved in 475 L of isopropyl alcohol and 25 L of mixed solution containing Nafion. Ni foam was broken up into 1 × 1 pieces and cleaned with acetone, ethanol, and DI water. The Ni foam substrate is coated with 4 L of the slurry, which was then dried at room temperature. The photoelectrochemical measurements were consisting of a working electrode, a saturated calomel electrode (SCE) is used as the reference

FIGURE 1 Schematic representation of Co-doped SrTiO₃ synthesis.

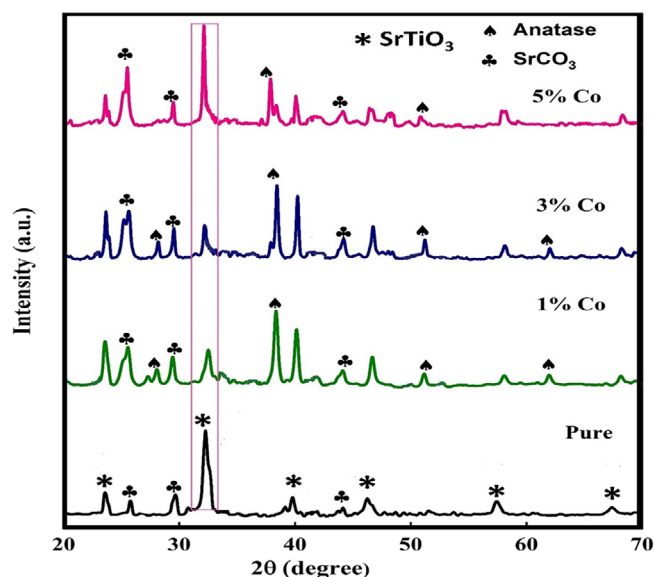
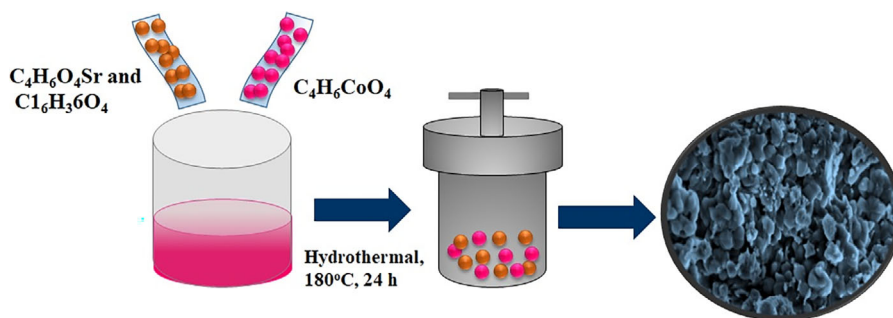


FIGURE 2 XRD analysis of pure SrTiO₃ and 1%, 3%, and 5% Co-doped SrTiO₃ samples.

electrode and graphite rod as counter electrode to measure the electrochemical properties. The electrochemical impedance spectroscopy (EIS) was studied by using Gamry 3000 potentiostat. Measurement has been done between 1 and 10 mHz on zero-volt DC bias potentials, which has been overlaid on 10 mV AC perturbation. Throughout, the measurement device has been kept on dark faradic cage to insure insulation from nearby electromagnetic fields.

3 | RESULTS AND DISCUSSION

3.1 | X-ray diffraction

The crystallite size of pure SrTiO₃ perovskite and cobalt doped nano powder SrTiO₃ have obtained from XRD analysis and drawn in Figure 2. The major peaks has been displayed at 22.6, 32.1, 39.6, 46.2, 57.3, and 67.3°, which has been assigned to (100), (110), (111), (200), (211), and (220), the peaks are all indexed to perovskite structure of SrTiO₃ which agree well with the data for the (JCPDS card No.- 893697).¹⁷ The diffraction peaks can be indexed as cubic SrTiO₃. Although some raw powders can still be seen in the final product as a second phase, it has been found that the main impurities are rutile

TiO₂ and SrCO₃ impurities. This demonstrates that drying causes more species to enter the pores, converting titania particles into anatase or rutile after calcination, while more Sr salt converts to SrCO₃ by absorbing CO₂ from the atmosphere. The XRD peaks intensities are decreased when the Co content was in a range of 1–3 wt %. An exception was that; a peak intensity was increased as the Co content was doped at 5 wt %. It was evident that different amounts of Co can be incorporated into the SrTiO₃ lattice. This may be attributed to the Co-induced change in the internal stress and surface energy during the growth of SrTiO₃. Also, Co ions may gradually occupy the regular as well as interstitial sites of SrTiO₃ ions at the Co doping concentrations from 1 to 3 wt %. At high concentration, 5 wt % of Co doping, Co ions would have occupied some additional interstitial sites, which are otherwise unoccupied. This effect would have led to the observed changes in the peak positions.¹⁸ For (110) plane Scherrer equation has been used to calculate crystallite size of pure SrTiO₃, which has been obtained around 41 nm when it is doped with 3% Cobalt ions, further decreases the crystallite size to 23 nm. It was observed that the crystallite size of the Co-doped SrTiO₃ nanoparticles decreased with an increasing content of Co doping except for the SrTiO₃ doping with 5 wt % Co. The decrease in the crystallite size of Co-doped SrTiO₃ nanoparticles is mainly attributed to the formation of Co-O-SrTi on the surface of the Co-doped SrTiO₃ nanoparticles. This can inhibit the crystal growth.

3.2 | FE-SEM

The morphology of pure SrTiO₃ and Co doped SrTiO₃ has been investigated using scanning electron microscopy. The synthesized pure SrTiO₃ nanoparticle shown in Figure 3 a are cubic in shape and partially agglomerated. FE-SEM images of 1%, 3%, and 5% Co-doped SrTiO₃ samples are shown in Figure 3 b–d. It has been evident from the images that introduction of cobalt improves the perovskite structure of the SrTiO₃ nanoparticles and suppress agglomeration.

3.3 | TEM analysis

The morphology of the synthesized SrTiO₃ and Co doped SrTiO₃ has been investigated TEM as well and shown in Figure 4. All the samples

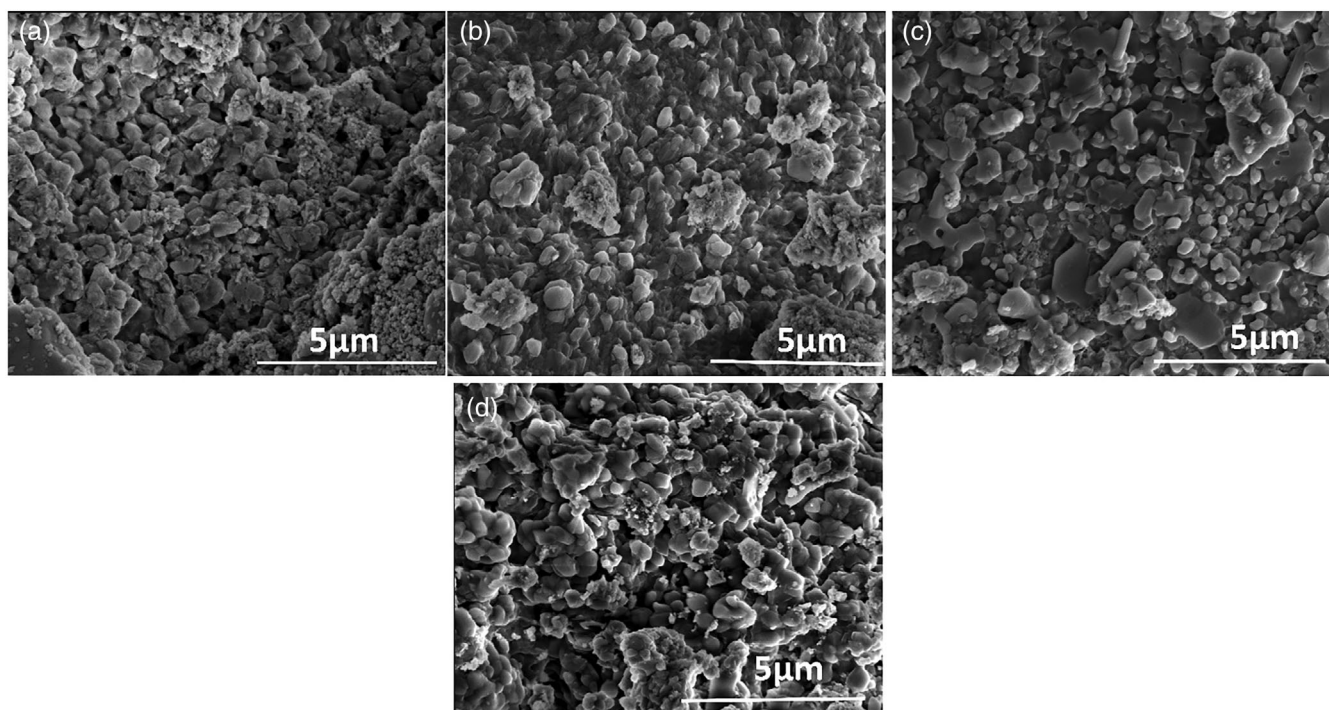


FIGURE 3 FE-SEM images of (a) pure SrTiO₃ (b) 1% Co-doped SrTiO₃, (c) 3% Co-doped SrTiO₃, (d) 5% Co-doped SrTiO₃.

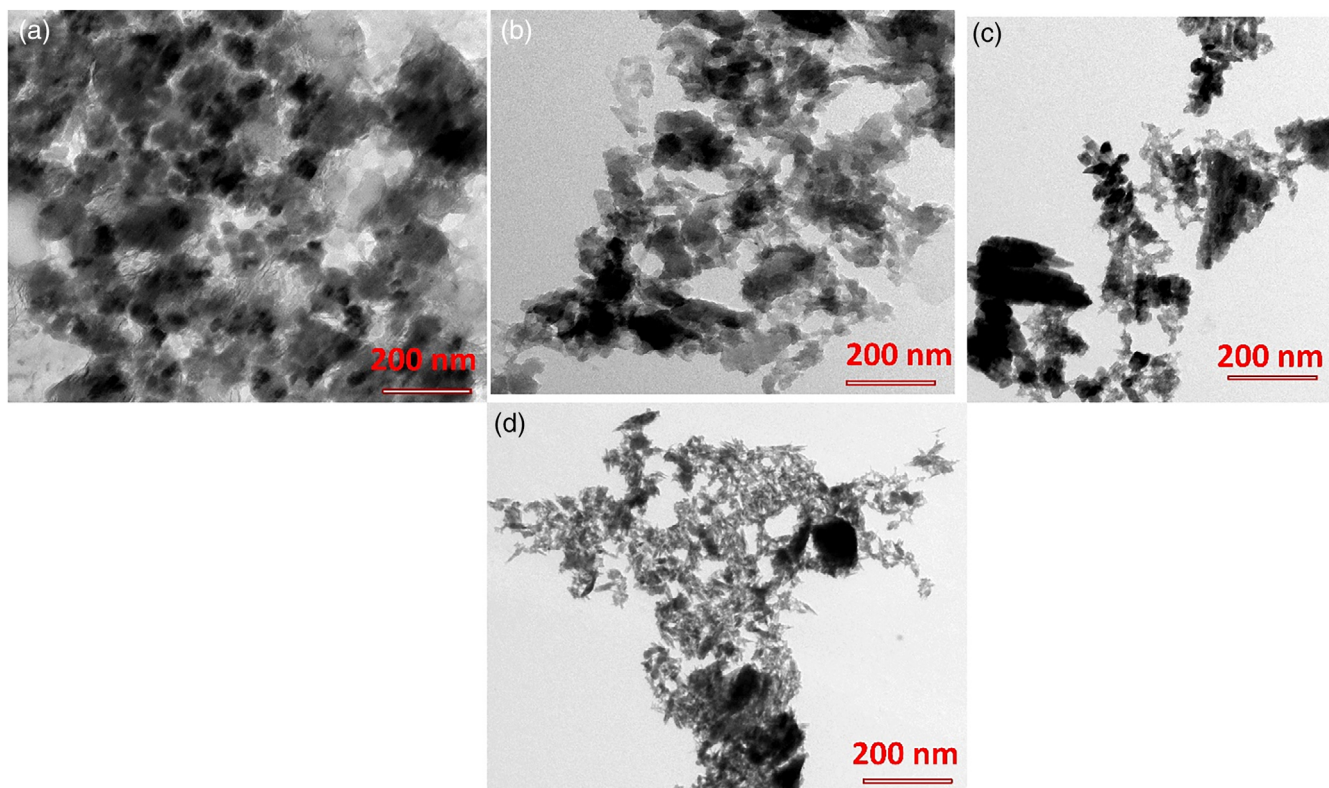
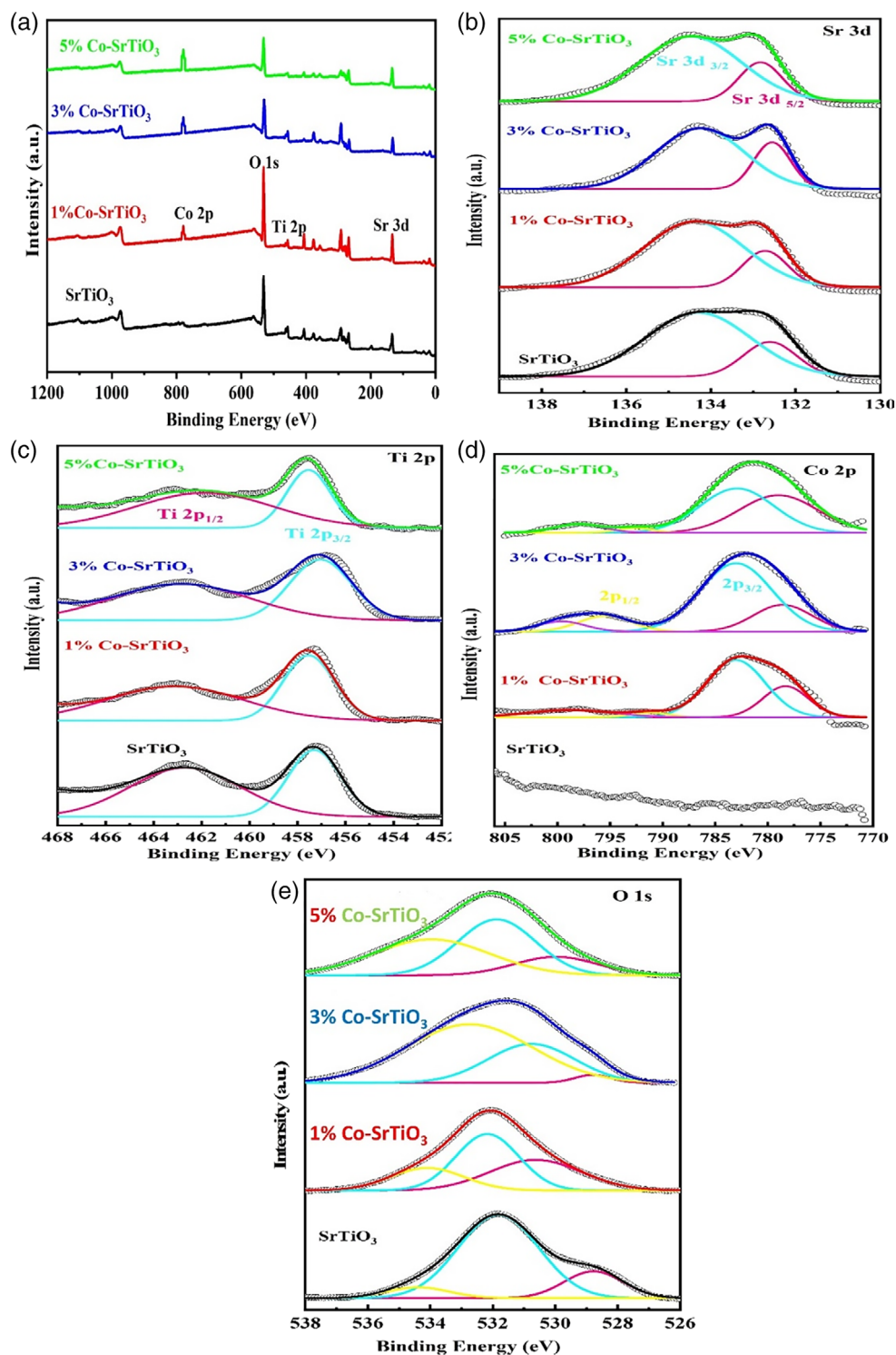


FIGURE 4 TEM images of (a) pure SrTiO₃ (b) 1% Co-doped SrTiO₃, (c) 3% Co-doped SrTiO₃, (d) 5% Co-doped SrTiO₃.

have shown agglomerated cubic in morphology. The introduction of Cobalt has reduced the particle size of the nanoparticle when compared with pure SrTiO₃. The mean diameter of pure SrTiO₃ and

Co/SrTiO₃ is approximately 40 and 25 nm respectively, this values are in good agreement with the crystallite size, which has been calculated from Scherrer equation with XRD results.

FIGURE 5 XPS spectra of pure SrTiO₃ and Co-doped SrTiO₃ samples (a) Wide survey spectra (b) Sr 3d, (c) Ti 2p, (d) Co 2p, and (e) O 1s.



3.4 | XPS analysis

For confirming surface chemical composition states of the SrTiO₃ perovskite and cobalt doped nano powder, XPS analysis has been performed. The wide survey spectrum of Figure 5 a indicates composition of nanocrystals including Sr, Ti, O in SrTiO₃ samples and Co for doped samples without other impurities. Figure 5 b indicates the Sr 3d_{5/2} and 3d_{3/2} peaks at 132.5 and 134.4 eV respectively, hence indicate

presence of Sr²⁺ state in all samples.¹⁹ The Ti matched with two peaks at 458.2 and 463.7 eV belongs with Ti element Ti 2p_{3/2} and Ti 2p_{1/2}.

The magnifying curve of cobalt shows two clearly visible peaks at 795 and 779, which contributed due to binding energies of Co 2p_{1/2} and Co 2p_{3/2} respectively. Furthermore these two peaks further split into individual two peaks around 795.9, 795.2, 780.2, and 779.1 eV.²⁰ The peaks at 795.9 and 780.2 assigned to Co³⁺ and the rest two

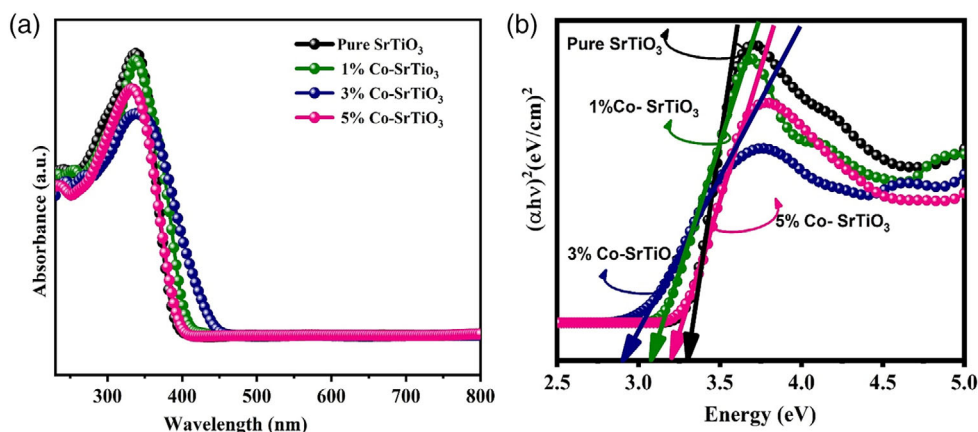


FIGURE 6 (a, b) Absorption spectra and Tauc's plot for the prepared samples.

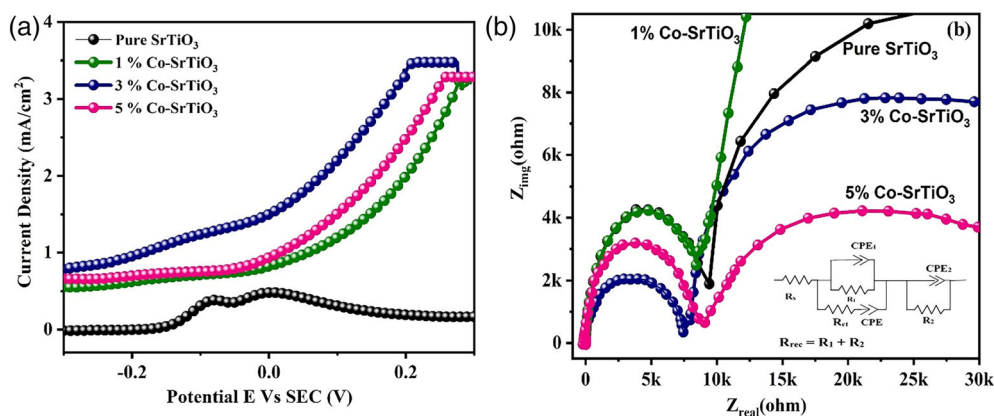


FIGURE 7 (a) LSV Polarization curve and (b) EIS spectra of pure SrTiO₃ Co-doped SrTiO₃ (Inset: RC Circuit used for the fitting of EIS raw data).

peaks at 795.2 and 779.1 has been assigned to Co²⁺ which proves that Co has been successfully doped to SrTiO₃ and the ion Co²⁺ and Co³⁺ both present in SrTi_{1-x}Co_xO₃.²¹ The O 1s high resolution XPS has been fitted with three Gaussian peaks around 529, 532.5, and 536 which can be described as, oxygen due to metal oxide, and presence of hydroxyl group at the surface and chemisorbed oxygen.²²

3.5 | Optical Analysis

UV-vis spectrophotometer was used to record the light absorption performance of samples. The optical absorption characteristics of pure SrTiO₃ and Co-doped SrTiO₃ are analyzed using UV-Vis diffuse reflectance spectra (DRS), as shown in Figure 6 a. Figure 6 b shows the spectra of Tauc's plot. Both pure and co-doped SrTiO₃ have exhibited absorption bands in the UV region at about 340 nm. The absorbance of Co-doped SrTiO₃ samples are shifted toward higher wavelength than pure SrTiO₃. There is a significant change for absorbance due to the introduction of cobalt ions into SrTiO₃ lattice.

As illustrated in Figure 5 b, the band gap of the prepared samples is calculated using Tauc's plots. The optical energy bandgap can be calculated from the x-axis intercept of extrapolating linear fit of a plot of $\ln(\alpha h\nu)^{1/2}$ versus $h\nu$. The calculated energy band gap values for pure SrTiO₃ and 1%, 3%, 5% Co-doped SrTiO₃ are found to be 3.29, 3.07, 2.90, and 3.20 eV.

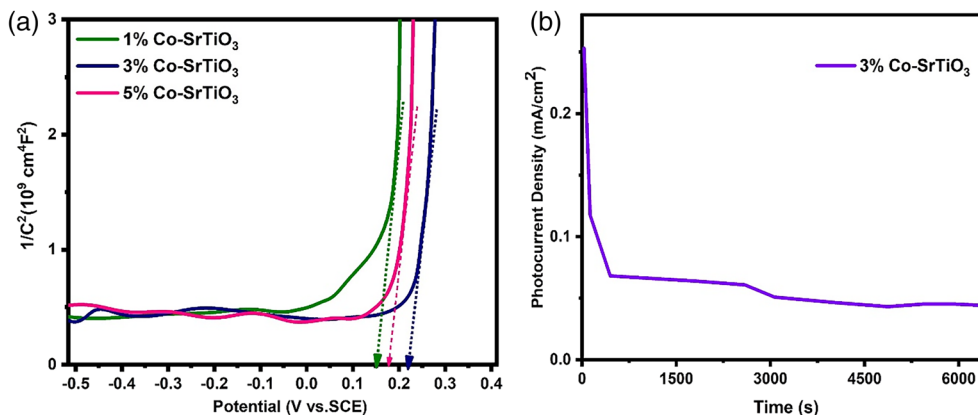
It is evident that as co-doping concentrations increase, the band gap slightly reduces. The change of SrTiO₃ lattice distortion may lead the band gap to shift. This could increase the number of defects in the SrTiO₃ lattice, which would alter light absorption and photocatalytic activity.

3.6 | Photo electrochemical properties

The Photo electrochemical (PEC) water splitting of the pure SrTiO₃ as well as (1%, 3%, and 5%) Co-doped SrTiO₃ samples were tested by linear sweep voltammetry (LSV) under simulated sunlight irradiation. As shown in Figure 7 a, it is clear that the photocurrent density is increased from 0.42 mA/cm² of pure SrTiO₃ to 3.45 mA/cm² for Co-doped SrTiO₃ photoanodes, indicating that the addition of cobalt can greatly improve the photoelectrochemical activity for the photoanodes. Due to the samples' increased active area and light absorption, the photocurrent density of the doped samples was increased. The cobalt doped SrTiO₃ samples has a stronger ability to capture visible light than the pure SrTiO₃ photocatalyst due to its narrow band gap compared to SrTiO₃ sample. An important factor that influences the sample's PEC performance is a surface defect such an oxygen vacancy²³ which provides very accessible sites for catalytic activities. In our case, the narrowing band gap and surface oxygen vacancy have an effect on the photoelectrochemical properties.

TABLE 1 Fitted EIS parameter for pure SrTiO₃ and Cobalt doped SrTiO₃.

		SrTiO ₃	1% Co-SrTiO ₃	3% Co-SrTiO ₃	5% Co-SrTiO ₃
R _{ct}	Light	12.23 kΩ	8.56 kΩ	7.56 kΩ	9.45 kΩ
	Dark	14.21 kΩ	9.26 kΩ	8.23 kΩ	11.21 kΩ

FIGURE 8 (a) Mott-Schottky plots and (b) Long-term stability curve.**TABLE 2** Photoelectrochemical performance of the Co-doped SrTiO₃ with literature reports.

Photocatalyst	Performance	Light Source	References
Co-doped SrTiO ₃	J = 3.45 mA/cm ²	300 W solar simulator	This work
BiVO ₄ /FeOOH/NiOOH	J = 2.73 mA/cm ²	150 W Xe lamp	25
CaFe ₂ O ₄	J = 110 μA/cm ²	500 W Xe lamp	26
Fe ₂ O ₃ /TiO ₂	J = 55 μA/cm ²	Xenon lamp (100 mW cm ⁻²)	27
α-Fe ₂ O ₃ /TiO ₂	J = 1.9 mA/cm ²	Xenon lamp (100 mW cm ⁻²)	28

The electrochemical behaviors of the composites have been studied using EIS technique. The charge transfers and recombination mechanisms have been explained using the equivalent RC circuit (Figure 7 b inset). Figure 7 b shows the Nyquist curve of the pure SrTiO₃, (1%, 3%, and 5%) Cobalt doped SrTiO₃ in 1 M KOH solution under light during the frequency range of 0.1 Hz to 100 kHz. The Nyquist curve shows two semi circles which belongs to charge transfer resistance (R_{ct}) and the parameter is shown in Table 1. The smallest R_{ct} have shown by the 3% Co doped SrTiO₃ which is required for better charge transfer. The Co doped composites have shown improved charge recombination behavior.²⁴

Figure 8a shows the 1/C² versus voltage plots (Mott-schottky) for 1%, 3%, and 5% Co-doped SrTiO₃ samples. The flat band potential is calculated using the Mott Schottky equation (V_{FB}). The V_{FB} can be calculated by extrapolating the linear portion of MS plots toward the x-axis. The obtained values for (1%, 3%, and 5%) Co-doped SrTiO₃ are 0.15, 0.17, 0.22 V, respectively. The positive shifting in the V_{FB} values is due to the convenient electron transfer and low recombination. Long-term stability of the photoanode is another criterion for realistic and large-scale H₂ generation; therefore, it is monitored for 2 h at 0 V. From the Figure 8 b, the photocurrent density of the as-prepared 3% Co-SrTiO₃ photoanode initially drops and then it is relatively constant over the extended period of time indicating good long-term stability. A comparison of the photoelectrochemical properties of present work with literature reports on the various photonode is given in Table 2.

4 | CONCLUSION

In this research work, we have successfully prepared pure SrTiO₃, 1% Cobalt doped SrTiO₃, 3% Cobalt doped SrTiO₃, 5% Cobalt doped SrTiO₃ photo catalysts using hydrothermal method. The prepared photo catalysts have been characterized for morphological study using FESEM and TEM. The SEM and TEM images of pure SrTiO₃ show nanoparticles are partially agglomerated. The introduction of Cobalt has reduced the particle size of the nanoparticle when compared with pure SrTiO₃. The mean diameter of pure SrTiO₃ and Co/SrTiO₃ is approximately 41 and 23 nm respectively and has been clearly shown through XRD that the profile of the peaks has been influenced by cubic as well as tetragonal phase. XPS analysis revealed purity and composition of the materials. The Electrochemical chemical impedance (EIS) spectroscopy showed that the prepared Co-SrTiO₃ composite have best charge transfer and recombination properties at 3% doping.

AUTHOR CONTRIBUTIONS

Arti Mishra: Data curation; formal analysis; methodology; writing – original draft. **Hemalatha Parangusan:** Data curation; formal analysis; methodology; writing – original draft. **Jolly Bhadra:** Conceptualization; supervision; validation; writing – review and editing. **Zubair Ahmed:** Conceptualization; supervision; validation; writing – review and editing. **Shoab Mallick:** Methodology. **Farid Touati:** Conceptualization; writing – review and editing. **Noora Al-Thani:** Funding acquisition; project administration; writing – review and editing.

ACKNOWLEDGMENTS

This publication was made possible by the support of an Qatar University Internal Grant (QUCG-CAM-20/21-6). The statements made herein are solely the responsibility of the authors. The characterizations of this work are accomplished in the Gas Processing Unit and in the Centra Laboratory Unit, at Qatar University.

CONFLICT OF INTEREST STATEMENT

The authors declare no conflicts of interest.

DATA AVAILABILITY STATEMENT

Data available on request from the authors: The data that support the findings of this study are available from the corresponding author upon reasonable request.

ORCID

Jolly Bhadra  <https://orcid.org/0000-0002-1350-6153>

REFERENCES

- Dong ZY, Yang J, Yu L, Daiyan R, Amal R. A green hydrogen credit framework for international green hydrogen trading towards a carbon neutral future. *Int J Hydrogen Energy*. 2022;47(2):728-734.
- Townsend TK, Browning ND, Osterloh FE. Nanoscale strontium Titanate Photocatalysts for overall water splitting. *ACS Nano*. 2012;6(8):7420-7426.
- Phoon BL, Lai CW, Juan JC, Show PL, Pan GT. Recent developments of strontium titanate for photocatalytic water splitting application. *Int J Hydrogen Energy*. 2019;44(28):14316-14340.
- Kageshima Y, Kawanishi T, Saeki D, Teshima K, Domen K, Nishikiori H. Boosted hydrogen-evolution kinetics over particulate lanthanum and rhodium-doped strontium Titanate Photocatalysts modified with phosphonate groups. *Angew Chem Int Ed*. 2021;60(7):3654-3660.
- Moniruddin M, Afroz K, Shabdan Y, Bizri B, Nuraje N. Hierarchically 3D assembled strontium titanate nanomaterials for water splitting application. *Appl Surf Sci*. 2017;419:886-892.
- Kavitha V et al. Optical and structural properties of tungsten-doped barium strontium titanate. *Mater Today Proc*. 2020;23:12-15.
- Lim PF, Leong KH, Sim LC, et al. Mechanism insight of dual synergistic effects of plasmonic Pd-SrTiO₃ for enhanced solar energy photocatalysis. *Appl Phys A*. 2020;126(7):550(1-10).
- Suzuki A, Oku T. Effects of transition metals incorporated into perovskite crystals on the electronic structures and magnetic properties by first-principles calculation. *Heliyon*. 2018;4(8):e00755.
- Guo Q, Li X, Wei H, Liu Y, et al. Sr, Fe Co-doped perovskite oxides with high performance for oxygen evolution reaction. *Front Chem*. 2019;7:224.
- Flores-Lasluisa JX, Huerta F, Cazorla-Amorós D, Morallón E. Structural and morphological alterations induced by cobalt substitution in LaMnO₃ perovskites. *J Colloid Interface Sci*. 2019;556:658-666.
- Tezcan F, Ahmad A, Yerlikaya G, Zia-ur-Rehman, Paksoy H, Kardaş G. The investigation of CdS-quantum-dot-sensitized Ag-deposited TiO₂ NRAs in photoelectrochemical hydrogen production. *New J Chem*. 2022;46(19):9290-9297.
- Mone P, Mardikar S, Balgude S. Morphology-controlled synthesis of Sn₃O₄ nanowires for enhanced solar-light driven photocatalytic H₂ production. *Nano-Structures & Nano-Objects*. 2020;24:100615.
- Xia Z, Yu R, Yang H, et al. Novel 2D Zn-porphyrin metal organic frameworks revived CdS for photocatalysis of hydrogen production. *Int J Hydrogen Energy*. 2022;47(27):13340-13350.
- Chen Y, Cheng Y, Zhao J, et al. Construction of Sb₂S₃/CdS/CdIn₂S₄ cascaded S-scheme heterojunction for improving photoelectrochemical performance. *J Colloid Interface Sci*. 2022;627:1047-1060.
- Liu C, Zhang C, Yin G, et al. A three-dimensional branched TiO₂ Photoanode with an ultrathin Al₂O₃ passivation layer and a NiOOH Cocatalyst toward Photoelectrochemical water oxidation. *ACS Appl Mater Interfaces*. 2021;13(11):13301-13310.
- Verma K et al. Magnetic field control of polarization/capacitance/voltage/resistance through lattice strain in BaTiO₃-CoFe₂O₄ multiferroic nanocomposite. *J Magn Magn Mater*. 2019;469:483-493.
- Ciobota CF, Piticescu RM, Neagoe C, et al. Nanostructured cobalt doped barium strontium Titanate thin films with potential in CO₂ detection. *Materials (Basel)*. 2020;13(21):4797(1-18).
- Ariyakkani P, Suganya L, Sundaresan B. Investigation of the structural, optical and magnetic properties of Fe doped ZnO thin films coated on glass by sol-gel spin coating method. *J Alloys Compd*. 2017;695:3467-3475.
- Ling J, Wang K, Wang Z, Huang H, Zhang G. Enhanced piezoelectric-induced catalysis of SrTiO₃ nanocrystal with well-defined facets under ultrasonic vibration. *Ultrason Sonochem*. 2020;61:104819.
- Li B, Wang C, Liu W, Zhong Y, An R. Synthesis of Co-doped barium strontium titanate nanofibers by sol-gel/electrospinning process. *Mater Lett*. 2012;75:207-210.
- Liu X, Gong H, Wang T, et al. Cobalt-doped perovskite-type oxide LaMnO₃ as Bifunctional oxygen catalysts for hybrid lithium-oxygen batteries. *Chem Asian J*. 2018;13(5):528-535.
- Ramos-Sanchez JE, Camposeco R, Lee SW, Rodríguez-González V. Sustainable synthesis of AgNPs/strontium-titanate-perovskite-like catalysts for the photocatalytic production of hydrogen. *Catal Today*. 2020;341:112-119.
- Andrei F, Boerasu I, Birjega R, et al. The effects of the oxygen content on the photoelectrochemical properties of LaFeO₃ perovskite thin films obtained by pulsed laser deposition. *Appl Phys A*. 2019;125(11):1-7.
- Echeverri E, Arnache O. Structural and impedance analysis of Co-doped SrTiO₃ perovskite. *J Phys Conf Ser*. 2016;687:012040.
- Kim TW, Choi K-S. Nanoporous BiVO₄ photoanodes with dual-layer oxygen evolution catalysts for solar water splitting. *Science*. 2014;343(6174):990-994.
- Ida S, Yamada K, Matsunaga T, Hagiwara H, Matsumoto Y, Ishihara T. Preparation of p-type CaFe₂O₄ photocathodes for producing hydrogen from water. *J Am Chem Soc*. 2010;132(49):17343-17345.
- Arifin K et al. TiO₂ doped with Fe₂O₃ for photoelectrochemical water splitting electrode: experimental and density functional theory study. *Malaysian J Anal Sci*. 2016;20(4):892-900.
- Deng J, Zhong J, Pu A, et al. Ti-doped hematite nanostructures for solar water splitting with high efficiency. *J Appl Phys*. 2012;112(8):084312.

SUPPORTING INFORMATION

Additional supporting information can be found online in the Supporting Information section at the end of this article.

How to cite this article: Mishra A, Parangusan H, Bhadra J, et al. Synthesis and photoelectrochemical performance of Co doped SrTiO₃ nanostructures photoanode. *Environ Prog Sustainable Energy*. 2023;e14186. doi:10.1002/ep.14186